

Diffusion-reaction modeling of silicon oxide interlayer growth during thermal annealing of high dielectric constant materials on silicon

Deepthi Gopireddy¹ and Christos G. Takoudis^{1,2,*}

¹*Advanced Materials Research Laboratory, Department of Chemical Engineering, University of Illinois at Chicago, Chicago, Illinois 60607, USA*

²*Department of Bioengineering, University of Illinois at Chicago, Chicago, Illinois 60607, USA*

(Received 12 November 2007; revised manuscript received 30 January 2008; published 5 May 2008)

We present the quantitative physicochemical modeling of the thermal annealing of high dielectric constant (k) thin films on silicon in oxygen and/or inert ambient. In particular, we study the kinetics of the SiO₂ interfacial layer growth at the high- k material structure/Si interface. Upon annealing, the transport of oxygen species in the high- k film to the silicon interface is quantitatively evaluated. One-dimensional unsteady-state diffusion-reaction equations are used to model the time evolution of the interfacial SiO₂ layer thickness. Because of the continuously increasing interfacial SiO₂ layer, the proposed model incorporates the moving interface that alters the diffusion length of the oxygen species. The numerical solution of the resulting modeling equations is based on the finite volume analysis method and it results in SiO₂ thickness profiles that comprise of an early fast growth stage followed by pseudosaturation into a self-limited regime. Our model predictions are found to satisfactorily agree with published experimental results. We also study the use of alumina as a potential oxygen diffusion barrier. Alumina is predicted to be an efficient barrier to oxygen diffusion, which is in agreement with published experimental data.

DOI: [10.1103/PhysRevB.77.205304](https://doi.org/10.1103/PhysRevB.77.205304)

PACS number(s): 77.55.+f

I. INTRODUCTION

There is an increasing effort to scale metal-oxide-semiconductor field effect transistor devices, particularly the gate insulator, to submicron levels with the aim of achieving higher device density. For the current materials of choice, silicon dioxide (SiO₂) and silicon oxynitrides (SiO_xN_y), gate oxide scaling is accompanied by an exponential increase in gate direct tunneling currents and an increase in source-drain leakage currents.^{1,2} The physical thickness limit of SiO₂ was estimated to be between 1.0 and 1.8 nm.²⁻⁴ Since current commercial devices incorporate gate oxide as thin as 2 nm, the continuous thinning of the gate dielectric forces the dielectric to operate close to its fundamental limit, thereby compromising the electrical properties and the reliability of the device. Moreover, decreasing lateral dimensions result in a reduction of the capacitance of the involved device. Therefore, in order to maintain the same gate capacitance, a thicker film with higher dielectric constant (k) is required to increase the effective area of each capacitor. Several candidate materials currently being investigated include Ta₂O₅,^{5,6} TiO₂,⁷ ZrO₂,^{8,9} HfO₂,¹⁰⁻¹³ Al₂O₃,¹⁴⁻¹⁹ etc. However, in order to evaluate these potential alternative high- k materials, it is essential to understand their compositional behavior and stability during further processing steps following high- k deposition on Si, more specifically thermal processing in inert and/or oxygen containing atmospheres. Since annealing in an oxygen ambient is an important step in forming the sidewalls of a complementary metal-oxide-semiconductor (CMOS) gate,²⁰ not only must the high- k material be thermodynamically stable on a Si substrate but also oxygen diffusion through the high- k film and oxygen reaction with the Si substrate must be controlled. Furthermore, previous studies have shown that postdeposition annealing of high- k films at moderate temperatures in oxygen can form an ultrathin SiO₂

layer that provides a high quality stable interface without significantly lowering the effective dielectric constant and decreases the susceptibility to hot electron injection due to lower electron barrier heights.^{11,21,22}

Although SiO₂ forms an ideal interface with Si, an uncontrollable amount of SiO₂ formation at the interface may lead to the formation of a dielectric stack associated with series capacitance that can significantly reduce the overall dielectric constant of the high- k structure. Thus, it is necessary to form a thin layer of SiO₂ that results in optimum electrical and structural properties at the interface while contributing to reducing interface trap density and leakage current. However, this precise control of the ultrathin SiO₂ layer formed as a function of annealing parameters remains a challenge. For this reason, knowledge of the transport mechanism of oxygen in the high- k material and its diffusion into the underlying substrate is crucial. While numerous studies have reported the use of gate stacks of high- k material and SiO₂, the objective of this work is to address a fundamental quantitative investigation of the transport of oxygen in the amorphous high- k material(s) deposited on Si substrates when submitted to annealing in dry oxygen and inert atmosphere and to provide a useful tool to make quantitative predictions of interface SiO₂ film thickness as functions of annealing parameters.

HfO₂/ZrO₂ have been shown to exhibit superior electrical characteristics compared to other alternative gate dielectrics; however, they have high oxygen diffusivities.^{10,23,24} HfO₂ along with ZrO₂ is reported to facilitate the fast transport of oxygen to the Si interface even at very low pressures.²⁰ Hence, there is a serious concern regarding control of the interface since any annealing treatments that have oxygen present may lead to rapid diffusion of oxygen through the high- k material, resulting in the formation of an uncontrolled amount of the SiO₂ interface layer. It is reported that oxygen

diffusion mechanisms in $\text{HfO}_2/\text{ZrO}_2$ and SiO_2 are quite different. In HfO_2 , oxygen diffusion occurs in atomic form through vacancies,^{20,25–27} while in SiO_2 , atomic oxygen has very low diffusion velocity and the oxidation of silicon implies reaction diffusion of molecular oxygen.^{4,28,29} Therefore, it was speculated that the silicon oxidation process in the presence of a HfO_2 layer can occur either through a complicated oxygen exchange mechanism at the $\text{HfO}_2/\text{SiO}_2$ interface^{30,31} or via the diffusion of either atomic oxygen into silicon oxide or molecular oxygen in HfO_2 .^{20,30,31} However, by using ^{18}O tracer in $\text{HfO}_2/\text{SiO}_2/\text{Si}$ stack, Ferrari and Fanciulli³² recently proposed that interface oxidation is caused by molecular O_2 diffusion throughout the entire $\text{HfO}_2/\text{SiO}_2$ stack and that such a diffusion process is limited by the low O_2 solubility in HfO_2 .

Deposited alumina films, on the other hand, are interesting because studies have shown excess oxygen in them rather than a stoichiometric amount.^{16–19} Therefore, annealing of these films even in an inert atmosphere leads to diffusion of the excess oxygen species to the Si interface to form the SiO_2 interfacial layer.¹⁶ Thus, oxygen species play a critical role in the diffusion-reaction mechanism during the thermal annealing process and consequently influence interface stability of high- k dielectrics.

In this study, we present the first quantitative description and solution of the diffusion-reaction problem of high- k nanostructures on silicon substrates; the unsteady-state nature of the underlying phenomena is explicitly recognized and accounted for. We use finite volume techniques to solve the resulting diffusion-reaction equations proposed for the diffusion of oxidant species through high- k materials, through the growing interfacial oxide, and the reaction to form silicon dioxide at the moving silicon oxide/silicon interface. By using the solutions to these equations, we are able to determine and quantitatively predict the growth kinetics of the SiO_2 interfacial layer at all times.

II. DIFFUSION REACTION

The thermal growth of a silicon oxide layer at the interface between a high- k material structure and the silicon substrate in a high- k/Si or high- $k/\text{SiO}_2/\text{Si}$ stack is modeled as a dynamic diffusion-reaction system capable of predicting and reproducing the observed profiles of diffusive oxygen front as well as its dependence on annealing parameters. The diffusing species is considered to be oxygen and the growth is the result of the reaction of oxygen with Si at the high- k/Si or SiO_2/Si interface. The overall growth kinetics can then be obtained at any temperature by specifying the diffusivity of oxygen species in the high- k material ($D_{\text{O,high } k}$) and in the growing SiO_2 ($D_{\text{O,SiO}_2}$), the rate constant of reaction between oxygen and Si, k_{SiO_2} , and the oxygen pressure in the gas phase. It is assumed that the SiO_2 layer growth is one dimensional, which is perpendicular to the face exposed to the ambient. The silicon diffusion through the SiO_2 film is neglected, which is in agreement with recent experimental results,³³ although subnanometer Si interstitial injection from the substrate may not be excluded. The additional assumptions made are that the diffusivity of oxygen species at a

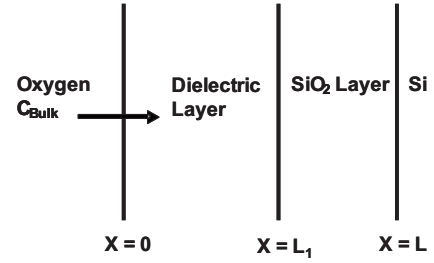


FIG. 1. Schematic of the diffusion-reaction process in high- k nanostructures.

certain temperature is constant, the density of the material in which diffusion occurs is constant and uniform, and the energy released by the oxidation reaction is rapidly dissipated so that the system remains in thermal equilibrium. Thus, the following process emerges (schematically shown in Fig. 1).

(1) The oxygen species are transported to the outer surface of the high- k layer from the bulk gas phase through a boundary layer.

(2) Oxygen species move inward into the metal-oxide film through diffusion.

(3) Upon reaching the bulk Si, they react to form a new interfacial layer of SiO_2 .

(4) As time proceeds, oxygen species diffuse through the metal-oxide structure, through the interfacial SiO_2 layer, reach Si interface, react, and produce more oxide, consequently pushing the SiO_2/Si interface further into the bulk Si region.

The one-dimensional mass balance diffusion equation for the description of the pathway of oxygen species through the high- k layer at an elapsed time (t) and location (x) can be expressed as follows:

$$\frac{\partial C_{\text{O,high } k}(x,t)}{\partial t} = D_{\text{O,high } k} \left(\frac{\partial^2 C_{\text{O,high } k}}{\partial x^2} \right), \quad 0 < x < L_1, \quad t \geq 0, \quad (1)$$

where $C_{\text{O,high } k}$ is the oxygen concentration in the high- k layer, $D_{\text{O,high } k}$ is the diffusion coefficient of oxygen in the high- k layer, and L_1 is the thickness of the high- k layer.

Once the oxygen reaches the high- k/Si interface, it irreversibly reacts with Si at the interface to form the SiO_2 layer. This reaction at the interface drives the oxygen diffusion at any instance of time and moves the Si interface boundary away from the initial position. The diffusing oxygen species now have to diffuse through the high- k layer and the newly formed SiO_2 layer to reach the interface. The diffusion of oxygen in the growing SiO_2 layer is given by the following mass balance equation:

$$\frac{\partial C_{\text{O,SiO}_2}(x,t)}{\partial t} = D_{\text{O,SiO}_2} \left(\frac{\partial^2 C_{\text{O,SiO}_2}}{\partial x^2} \right), \quad L_1 < x < L, \quad t > 0, \quad (2)$$

where $C_{\text{O,SiO}_2}$ is the concentration of oxygen species in the SiO_2 layer, $D_{\text{O,SiO}_2}$ is the diffusion coefficient of oxygen spe-

cies in the SiO_2 layer, and L is the thickness of high- k plus SiO_2 layers at time t .

Initially, the distribution of oxygen species is assumed to be homogeneous in the high- k layer, i.e., at $t=0$. Therefore, the initial conditions can be written as

$$C_{\text{O,high } k} = C_{\text{O}}, \quad 0 \leq x \leq L_1, \quad t = 0, \quad (3)$$

$$C_{\text{O,SiO}_2} = 0, \quad x = L, \quad t = 0, \quad (4)$$

where C_0 is the initial concentration of (excess) oxygen species in the dielectric layer.

Considering a simple situation of the initial surface exposed to uniform oxygen environment, the boundary condition at $x=0$ becomes

$$-D_{\text{O,high } k} \frac{\partial C_{\text{O,high } k}}{\partial x} = h(C_{\text{bulk}} - C_{\text{O,high } k}), \quad x = 0, \quad t > 0, \quad (5)$$

where h is the mass transfer coefficient. Equation (5) shows that the concentration at the surface ($x=0$) is governed by mass transfer through a thin film of oxygen formed at the surface. The mass transfer coefficient is solely determined by a gas-phase transport process; its value can be estimated on the basis of standard boundary conditions and the contribution of the gas-phase transport to the overall diffusion-reaction process of these systems is relatively small.²⁸

The formation of SiO_2 causes a discontinuity at the high- k / SiO_2 interface due to the different diffusivities of oxygen in these two layers. However, continuity of flux, i.e., that no accumulation of the diffusing oxygen at the high- k / SiO_2 interface, results in the following mass balance equation at $x=L_1$:

$$D_{\text{O,high } k} \left(\frac{\partial C_{\text{O,high } k}}{\partial x} \right) = D_{\text{O,SiO}_2} \left(\frac{\partial C_{\text{O,SiO}_2}}{\partial x} \right), \quad x = L_1, \quad t > 0. \quad (6)$$

At the Si/high- k material structure interface, the flux corresponding to the oxidation reaction with first order rate constant k_{SiO_2} results in the following:

$$-D_{\text{O,high } k} \frac{\partial C_{\text{O,high } k}(x)}{\partial x} = k_{\text{SiO}_2} C_{\text{O,high } k}, \quad x = L_1, \quad t = 0 \quad (7)$$

and

$$-D_{\text{O,SiO}_2} \frac{\partial C_{\text{O,SiO}_2}(x)}{\partial x} = k_{\text{SiO}_2} C_{\text{O,SiO}_2}, \quad x = L, \quad t > 0. \quad (8)$$

The flux of formation of SiO_2 is equal to the reactive flux at the Si interface ($x=L$). Therefore, if N_1 is the number of oxidant molecules incorporated into a unit volume of the oxide layer as suggested by Deal and Grove,²⁸ the rate of growth of the oxide layer can be described by the following equation:

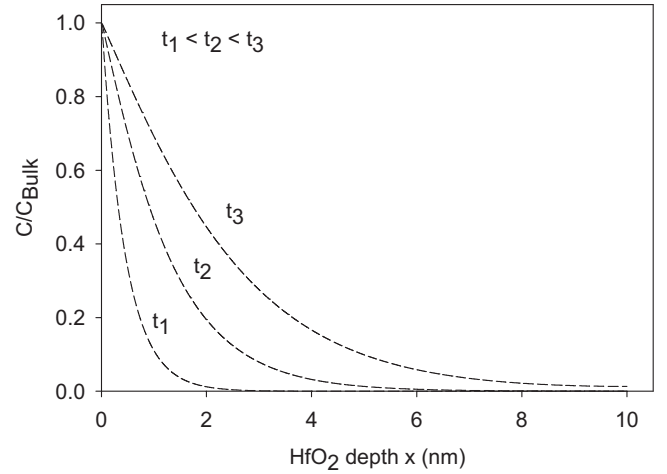


FIG. 2. Predicted oxygen concentration profiles in a 10 nm thick HfO_2 dielectric layer for different oxidation times at 900 °C and 1 bar O_2 . The values used are $D_{(\text{O}_2, \text{HfO}_2)} = 201.6 \text{ nm}^2/\text{s}$ (Refs. 30 and 35), $D_{(\text{O}_2, \text{SiO}_2)} = 2.5 \times 10^4 \text{ nm}^2/\text{s}$ (Ref. 36), $k_{(\text{SiO}_2)} = 641.8 \text{ nm}/\text{s}$ (Ref. 36), $\bar{h} = 2.8 \times 10^7 \text{ nm}/\text{s}$ (Ref. 28), $C_0 = 0$, and $C_{\text{bulk}} = 0.0062 \text{ molecules}/\text{nm}^3$ (calculated by using ideal gas equation).

$$\frac{dx}{dt} = \frac{k_{\text{SiO}_2} C_{\text{O,SiO}_2}}{N_1}, \quad x = L, \quad t > 0. \quad (9)$$

The above balance equations along with their corresponding boundary and initial conditions are solved by using the finite volume approach described by Pantankar³⁴ to yield concentration profiles with suitable values for the system parameters. The partial differential equations are changed to form a set of linear algebraic equations by dividing both space and time into discrete intervals. A control volume approach is used to replace the continuous information in the exact solution of the partial differential equation with discrete values, while the time dependency is resolved by using a fully sufficient fixed time step.³⁴ The control volume method naturally maintains conservation of species and rigorously handles the discontinuities due to the heterogeneous material properties. The resulting sparse linear set of equations is solved by using a tridiagonal matrix algorithm in MATLAB.

III. RESULTS AND DISCUSSION

A. Hafnium oxide film on silicon substrates

When HfO_2 is used as the dielectric material and there is *a priori* knowledge of the values of $D_{\text{O,high } k}$, $D_{\text{O,SiO}_2}$, h , C_{bulk} , C_0 , and $k_{\text{O,SiO}_2}$, the concentration profiles and growth kinetics can be achieved at each space and time interval. Unfortunately, good values of $D_{\text{O,high } k}$, $D_{\text{O,SiO}_2}$, h , C_0 , and $k_{\text{O,SiO}_2}$ for high- k materials are not readily available. However, the numerical solutions are obtained by using values based on literature and the nature of the physicochemical system of interest.

Predicted diffusive oxygen concentration depth profiles through a 10 nm thick HfO_2 film at 1 bar O_2 and 900 °C are illustrated in Fig. 2 for different growth times. The parameter values used are $D_{(\text{O}_2, \text{HfO}_2)} = 201.6 \text{ nm}^2/\text{s}$,^{30,35} $D_{(\text{O}_2, \text{SiO}_2)} = 2.5$

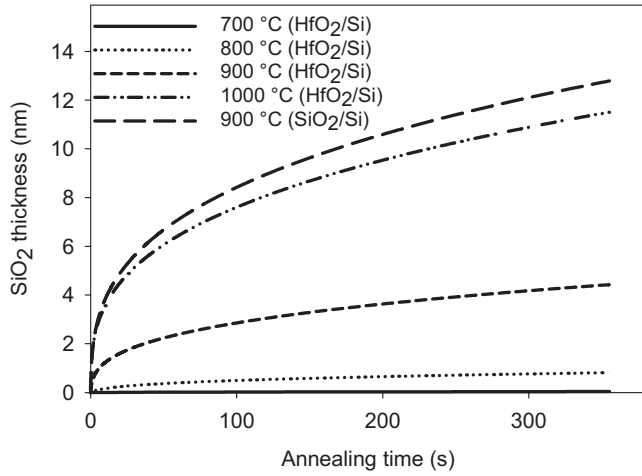


FIG. 3. Predicted thickness of interlayer SiO_2 film as a function of annealing time on 10 nm thick HfO_2 on SiO_2 at 1 bar O_2 and annealing temperatures of 700, 800, 900, and 1000 °C. Also, the growth of SiO_2 on bare silicon is shown as a function of time at 900 °C and 1 bar O_2 . In this simulation, we used $D_{(\text{O}_2, \text{HfO}_2)} = 4.82 \times 10^{10} \exp[-22\,629.68/T(\text{K})] \text{ nm}^2/\text{s}$ (Refs. 30 and 35), $D_{(\text{O}_2, \text{SiO}_2)} = 1.3 \times 10^{13} \exp[-23\,568.2/T(\text{K})] \text{ nm}^2/\text{s}$ (Ref. 36), $k_{(\text{SiO}_2)} = 2.45 \times 10^{14} \exp[-31\,281.5/T(\text{K})] \text{ nm/s}$ (Ref. 36), $h = 2.8 \times 10^7 \text{ nm/s}$ (Ref. 28), $C_0 = 0$, and $C_{\text{bulk}} = 0.0062 \text{ molecules/nm}^3$ (calculated by using ideal gas equation).

$\times 10^4 \text{ nm}^2/\text{s}$,³⁶ $k_{(\text{SiO}_2)} = 641.8 \text{ nm/s}$,³⁶ $h = 2.8 \times 10^7 \text{ nm/s}$,²⁸ $C_0 = 0$ (i.e., stoichiometric HfO_2 film), and $C_{\text{bulk}} = 0.0062 \text{ molecules/nm}^3$ (calculated using the ideal gas equation). For this particular system, we assume that there is no initial SiO_2 layer present at the high- k/Si interface. One can see that oxygen species diffuse into the high- k layer, arriving at the high- k/Si interface to react with Si. The oxygen profiles are not straight lines and this is the result of the dynamic nature of the diffusion-reaction problem in these systems. However, for long enough annealing times, the oxygen concentration profile asymptotically approaches a straight line. A steady-state regime is not attained as long as the SiO_2/Si interface moves deeper into the Si substrate.

Figure 3 illustrates the predicted interfacial oxide thickness as a function of annealing time of a 10 nm thick HfO_2 on silicon at different annealing temperatures and 1 bar pure oxygen. The rate of SiO_2 formation on bare silicon substrate at 900 °C and 1 bar oxygen is also plotted for comparison. The values used are $D_{(\text{O}_2, \text{HfO}_2)} = 4.82 \times 10^{10} \exp[-22\,629.68/T(\text{K})] \text{ nm}^2/\text{s}$,^{30,35} $D_{(\text{O}_2, \text{SiO}_2)} = 1.3 \times 10^{13} \exp[-23\,568.2/T(\text{K})] \text{ nm}^2/\text{s}$,³⁶ $k_{(\text{SiO}_2)} = 2.45 \times 10^{14} \exp[-31\,281.5/T(\text{K})] \text{ nm/s}$,³⁶ $h = 2.8 \times 10^7 \text{ nm/s}$,²⁸ $C_0 = 0$, and $C_{\text{bulk}} = 0.0062 \text{ molecules/nm}^3$. It is apparent that Si at the high- k/Si interface is initially consumed by reaction with the diffusing O_2 species to form silicon oxide, and as processing time proceeds, the reaction front advances into the Si matrix. The interfacial SiO_2 layer therefore becomes thicker with increasing annealing time. The growth kinetics is faster during the early stage of annealing, e.g., within the first 10 s, the SiO_2 thickness increases from 0 to 1.3 nm when annealed at 900 °C, followed by a rapid change into a slower, apparently self-limited growth regime that lasts for long process-

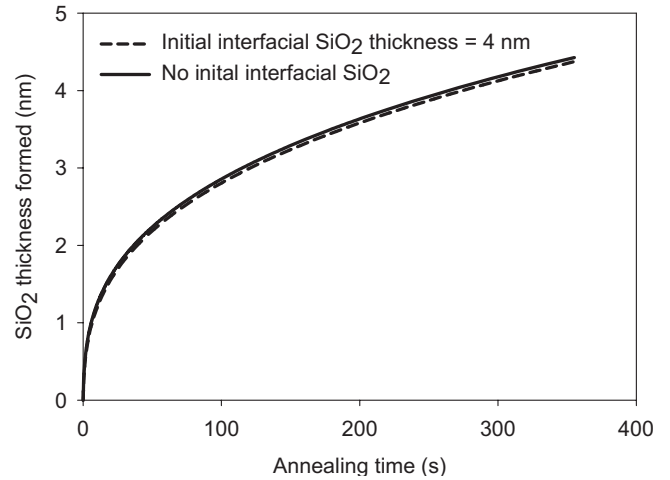


FIG. 4. Comparison of SiO_2 film thickness formed at the interface without initial oxide present and when an initial oxide of 4 nm is present, at 900 °C and 1 bar O_2 ambient. The values used in these modeling predictions are $D_{(\text{O}_2, \text{HfO}_2)} = 201.6 \text{ nm}^2/\text{s}$ (Refs. 30 and 35), $D_{(\text{O}_2, \text{SiO}_2)} = 2.5 \times 10^4 \text{ nm}^2/\text{s}$ (Ref. 36), $k_{(\text{SiO}_2)} = 641.8 \text{ nm/s}$ (Ref. 36), $h = 2.8 \times 10^7 \text{ nm/s}$ (Ref. 28), $C_0 = 0$, and $C_{\text{bulk}} = 0.0062 \text{ molecules/nm}^3$ (calculated by using ideal gas equation).

ing times even at high annealing temperatures. For annealing temperatures below ~ 800 °C, the interlayer growth rate is fairly small and the maximum oxide thickness is predicted to be 1 nm or less. At higher annealing temperatures, the predicted interfacial oxide thickness is found to significantly increase with increasing annealing temperature.

Next, we investigate the interfacial layer growth in order to understand the limiting step that is responsible for the apparent self-limited growth kinetics at longer annealing times. We consider the following processes that form the basis of our model: (1) incorporation of oxygen into HfO_2 , (2) diffusion of oxygen species in the HfO_2 dielectric layer, (3) diffusion of oxygen species in the interfacial SiO_2 layer, and (4) reaction of oxygen with silicon at the interface. The oxidation reaction rate at the Si interface is considered first. Shimizu *et al.*³¹ have reported that the oxidation reaction at the HfO_2/Si interface is independent of the Si substrate surface orientation. This is contrary to the bare Si surface oxidation in which the surface orientation has an effect on the SiO_2 growth rate.^{31,37} These findings indicate that the oxidation reaction at the Si interface is fast and likely not the limiting process for interfacial oxide growth. The interfacial SiO_2 layer growth and its effect on the overall growth kinetics are considered next. The interlayer growth with no initial silicon oxide as well as with an initial predeposited silicon oxide of 4 nm thick are modeled, and the resulting equations are solved with the parameter values of $D_{(\text{O}_2, \text{HfO}_2)} = 201.6 \text{ nm}^2/\text{s}$,^{30,35} $D_{(\text{O}_2, \text{SiO}_2)} = 2.5 \times 10^4 \text{ nm}^2/\text{s}$,³⁶ $k_{(\text{SiO}_2)} = 641.8 \text{ nm/s}$,³⁶ $h = 2.8 \times 10^7 \text{ nm/s}$,²⁸ $C_0 = 0$, and $C_{\text{bulk}} = 0.0062 \text{ molecules/nm}^3$ (calculated by using the ideal gas equation for 1 bar oxygen and 900 °C). The resulting interlayer thicknesses as functions of the annealing time are shown in Fig. 4; it is evident that the predicted trends for the annealing of HfO_2 layers deposited with and without pre-

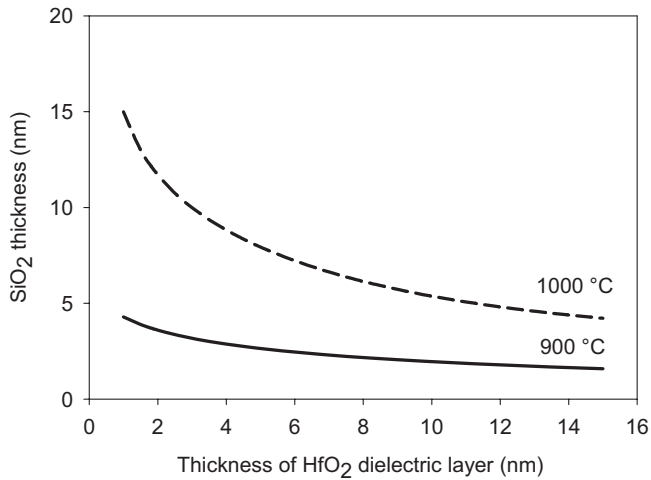


FIG. 5. Thickness of the interfacial SiO_2 film as a function of dielectric thickness at 1 bar O_2 and annealing temperatures of 900 and 1000 °C for 35 s. In these theoretical predictions, we used $D_{(\text{O}_2, \text{HfO}_2)} = 4.82 \times 10^{10} \exp[-22\,629.68/T(\text{K})] \text{ nm}^2/\text{s}$ (Refs. 30 and 35), $D_{(\text{O}_2, \text{SiO}_2)} = 1.3 \times 10^{13} \exp[-23\,568.2/T(\text{K})] \text{ nm}^2/\text{s}$ (Ref. 36), $k_{(\text{SiO}_2)} = 2.45 \times 10^{14} \exp[-31\,281.5/T(\text{K})] \text{ nm/s}$ (Ref. 36), $h = 2.8 \times 10^7 \text{ nm/s}$ (Ref. 28), $C_0 = 0$, and $C_{\text{bulk}} = 0.0062 \text{ molecules/nm}^3$ (calculated by using ideal gas equation).

grown silicon oxide are found to be quantitatively similar to each other. This suggests that the formation of interfacial oxide layer does not significantly inhibit the diffusion of oxygen species and, therefore, it may not have a significant effect on the overall interlayer film growth. Moreover, in Fig. 3, the SiO_2 growth kinetics on bare silicon modeled at the same conditions as those of the HfO_2 film on Si shows that for longer annealing times, the oxide growth on bare silicon is much faster. It is known that diffusion of molecular oxygen in SiO_2 is fast. Therefore, the lower thicknesses of the silicon dioxide interlayer than those of SiO_2 formed on bare silicon under similar conditions can be explained by the lower diffusivity of molecular oxygen through the dielectric layer; this slower diffusion of oxygen in the high- k layer can therefore become the rate limiting step.

The effect of the rate of oxygen diffusion through the HfO_2 layer as the limiting process on the overall growth kinetics of the interlayer silicon oxide film is investigated too. Figure 5 shows the predicted interfacial SiO_2 growth at two different annealing temperatures in 1 bar oxygen for 35 s as a function of the initial HfO_2 film thickness; the parameter values used are the same as those mentioned above at the appropriate temperatures. In the ultrathin HfO_2 region, the interface silicon oxide layer growth is predicted to decrease with increasing HfO_2 thickness, which prevents progressive incorporation of O_2 species at the SiO_2/Si interface and consequently slows down film growth. This suggests that when a very thin HfO_2 layer is used, the oxygen species diffusion through the dielectric is likely the limiting step. However, small HfO_2 thickness dependence of the silicon oxide interlayer thickness is observed at the temperatures studied for relatively thick ($>4 \text{ nm}$) dielectric layers. As the thickness of the high- k material on Si increases, the diffusion of the molecular oxygen species through the developing di-

electric stack becomes overall rate controlling, due to the diffusion barrier presented by the dielectric layer. This does not appear to be in agreement with results reported by other groups,^{30,31,35} which indicated that the interfacial Si oxidation process may not be limited by the diffusion of oxygen through the developing dielectric stack. Yet, possible oxygen isotopic exchange, the reporting of the diffusing species being mostly atomic oxygen, and the remarkable agreement between our theoretical predictions and the data presented in Ref. 29 (see below) suggest that our proposed physicochemical model with molecular oxygen being the diffusing species throughout the $\text{HfO}_2/\text{SiO}_2$ stack³² is a satisfactory and effective representation of the unsteady-state oxygen diffusion-reaction phenomena in high dielectric constant material structures. Further, the interface SiO_2 growth was modeled for different oxygen partial pressures (not shown). The results agree with published data that small oxygen partial pressure dependence is observed for the growth of interfacial SiO_2 . This not only suggests that incorporation of oxygen species into the HfO_2 layer does not limit the oxidation reaction at the interface but also that oxygen diffusion through the dielectric layer is most likely the limiting process.

In order to assess the effectiveness of the model in describing the oxide growth not only qualitatively but also quantitatively, theoretically predicted results must be compared to experimental evidence. Data obtained by Ferrari and Scarel³⁰ were used. A relatively thin native oxide film thickness ($\sim 1.2 \text{ nm}$) was used as the initial SiO_2 thickness at the interface. The parameter values used are $D_{(\text{O}_2, \text{HfO}_2)} = 201.6 \text{ nm}^2/\text{s}$,^{30,35} $D_{(\text{O}_2, \text{ZrO}_2)} = 250.6 \text{ nm}^2/\text{s}$,^{20,25,30} $D_{(\text{O}_2, \text{SiO}_2)} = 2.5 \times 10^4 \text{ nm}^2/\text{s}$,³⁶ $k_{(\text{SiO}_2)} = 641.8 \text{ nm/s}$,³⁶ $h = 2.8 \times 10^7 \text{ nm/s}$,²⁸ $C_0 = 0$, and $C_{\text{bulk}} = 0.0062 \text{ molecules/nm}^3$. In Fig. 6, predicted values of the interlayer silicon oxide thickness for the fast growth early on up to the self-limited regime at longer annealing times are presented and found to satisfactorily agree with those published experimental data for both 10 nm thick HfO_2 and 10 nm thick ZrO_2 films. Indeed, the presence of the $\text{HfO}_2/\text{ZrO}_2$ layer on silicon is seen to result in a steep increase of the interfacial layer to about 3 nm, while for longer annealing times, the growth of interlayer SiO_2 proceeds at a much slower rate.

Another metric that can be used to define a high- k film is the equivalent oxide thickness (EOT), which is the thickness of a SiO_2 film with equivalent capacitance. It is crucial that EOT values be as low as possible while maintaining a physical thickness large enough to prevent leakage currents. In order to incorporate a high- k film into a CMOS structure, the EOT should be less than 1.5 nm for a sub-100-nm device. Therefore, if 4 nm HfO_2 ($\epsilon = 25$) is used as the dielectric layer, the annealing time must be shorter than 1.5 s at 900 °C. The EOT values calculated from our model can be compared to electrically measured values of 2.5 nm for a 4 nm thick HfO_2 with 1 nm initial SiO_2 film annealed in oxygen at 1000 °C for 1 s.³⁸ The predicted EOT value, which is calculated by using $\epsilon(\text{HfO}_2) = 25$ and $\epsilon(\text{SiO}_2) = 3.9$, is 2.77 nm. The small difference between the predicted and experimental values may be attributed to the interfacial oxide's silicate component due to high temperature annealing. Because our model does not account for silicate formation and since the total capacitance of a multilayer stack is affected by

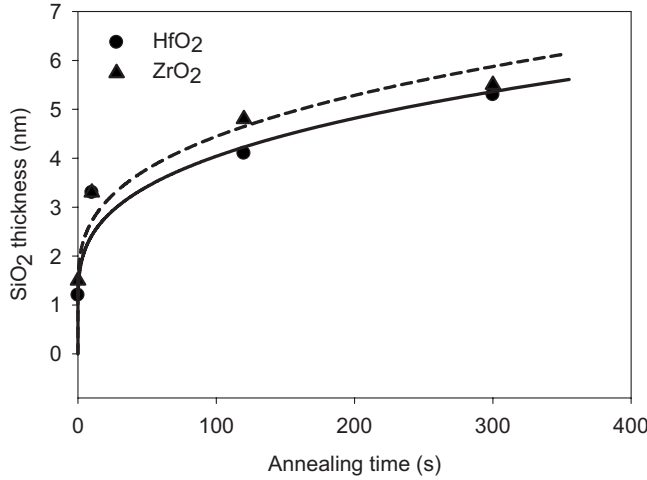


FIG. 6. Predicted thickness of the interlayer SiO_2 film as a function of annealing time of 10 nm thick HfO_2 (—) and 10 nm thick ZrO_2 (- -) at 1 bar O_2 and 900 °C along with the corresponding experimental data from Ferrari and Scarel (Ref. 30). The parameters used are $D_{(\text{O}_2, \text{HfO}_2)}=201.6 \text{ nm}^2/\text{s}$ (Refs. 30 and 35), $D_{(\text{O}_2, \text{ZrO}_2)}=250.6 \text{ nm}^2/\text{s}$ (Refs. 20, 25, and 30), $D_{(\text{O}_2, \text{SiO}_2)}=2.5 \times 10^4 \text{ nm}^2/\text{s}$ (Ref. 36), $k_{(\text{SiO}_2)}=641.8 \text{ nm}/\text{s}$ (Ref. 36), $h=2.8 \times 10^7 \text{ nm}/\text{s}$ (Ref. 28), $C_0=0$, and $C_{\text{bulk}}=0.0062 \text{ molecules}/\text{nm}^3$ (calculated by using ideal gas equation).

the material with a lower dielectric constant (dielectric constant for Hf silicate <25), our model predicts a slightly higher value for EOT. However, our model can be modified to consider Si migration to the dielectric layer resulting in silicate layer formation.

Previous studies have shown that annealed ZrO_2 and HfO_2 films contain a significant amount of Si.³⁰ When the SiO_2 interface layer is formed, it occupies a large volume generating interstitial Si that is prone to move. This interstitial Si migrates toward the dielectric layer and reacts to form a Hf-O-Si (Zr-O-Si) structure or a SiO_2 - HfO_2 (SiO_2 - ZrO_2) phase mixture. This phenomenon can be incorporated into our model by using the following diffusion-reaction equations to describe the Si migration and silicate formation:

$$\frac{\partial C_{\text{Si}}(x,t)}{\partial t} = D_{\text{Si}} \left(\frac{\partial^2 C_{\text{Si}}}{\partial x^2} \right) + k_{\text{SiO}_2} C_{\text{O}, \text{SiO}_2} - k_{\text{Si-high } k} C_{\text{Si}} C_{\text{high } k}, \quad (10)$$

$$\frac{\partial C_{\text{high } k}(x,t)}{\partial t} = -k_{\text{Si-high } k} C_{\text{Si}} C_{\text{high } k}, \quad (11)$$

where C_{Si} is the concentration of interstitial Si formed, $C_{\text{high } k}$ is the concentration of the high- k material that reacts with Si, D_{Si} is the diffusion coefficient of Si, and $k_{\text{Si-high } k}$ is the rate constant for silicate formation.

By using appropriate boundary conditions, Eqs. (1)–(11) can be numerically solved to describe the time evolution of both Si and O species. Additionally, the annealing temperature plays an important role since high temperature annealing can induce film crystallization, creating preferential diffusion paths. It has been shown that upon annealing, amorphous HfO_2 crystallizes into monoclinic phase, while ZrO_2 is com-

posed of a mixture of amorphous, monoclinic, and tetragonal phases.²⁰ Therefore, transport of oxygen species through the film can be via bulk diffusion or grain boundary diffusion or a combination of both. It is likely that the occurrence of the above processes influences the interfacial layer growth process, either by modifying oxygen diffusivity and reactivity with Si or, in the case of Si diffusion, changing the composition of the dielectric and interface layers. However, given the complexity of the phenomena occurring simultaneously, we have derived a comprehensive model, which highlights the important variables for the interface layer growth and the mechanism of oxygen transport.

B. Alumina film on silicon substrates

Aluminum oxide has attracted considerable interest, primarily due to its potential to replace SiO_2 as the dielectric layer in CMOS device fabrication. Among its desirable properties, the most noteworthy one is the ability of stoichiometric Al_2O_3 to form a thermodynamically stable interface with Si. This is a considerable advantage because the dielectric-substrate interface in a field effect transistor device must be of high quality. However, the O/Al ratio of ultrathin ($<10 \text{ nm}$) aluminum oxide films obtained by different deposition processes currently employed, depends on the process and it may be considerably higher than the stoichiometric one in Al_2O_3 .^{16–19} This results in the formation of a SiO_2 layer at the $\text{Al}_2\text{O}_3/\text{Si}$ interface during annealing even in inert ambient, and it can be explained by the possible diffusion of the excess oxygen species present in the film toward the substrate along with the resulting reaction at the substrate interface to form SiO_2 . Such observations indicate that there are interesting design issues in the use of Al_2O_3 as a high- k material and that an understanding of the mechanism of the formation of the silicon oxide interlayer is necessary for the application of such systems as ultrathin dielectrics.

The lack of information for the exact nature of the diffusing species poses a considerable challenge in deriving a detailed fundamental analysis of the system. Considering that the interfacial oxide formation occurs even after annealing at 500 °C in argon gas, the diffusing species is apparently highly reactive.¹⁶ One plausible mechanism is the diffusion of atomic oxygen from the oxygen rich alumina film followed by reaction at the film/substrate interface to form SiO_2 . In an alternative mechanism, the excess diffusive oxygen is exchanged for the fixed oxygen already present in the Al_2O_3 network. As a result, a fraction of diffusive oxygen displaces the fixed oxygen, generating another oxygen species. Upon reaching the silicon interface, the oxygen species reacts with Si. In our physicochemical model, we consider that the deposited film contains excess oxygen (C_0) and a fraction of the excess oxygen (α) diffuses in the film with an effective diffusivity ($D_{\text{O}, \text{Al}_2\text{O}_3}$). The excess oxygen species in our modeling studies is based on the stoichiometry of the deposited alumina as $\text{AlO}_{2.1 \pm 0.1}$ (Ref. 16); other parameters used are 1 bar of argon, 500 °C, $D_{(\text{O}_2, \text{SiO}_2)}=25.0 \text{ nm}^2/\text{s}$,³⁶ $k_{(\text{SiO}_2)}=0.035 \text{ nm}/\text{s}$,³⁶ $h=2.8 \times 10^7 \text{ nm}/\text{s}$,²⁸ and $C_0=11.7 \text{ molecules}/\text{nm}^3$. The fit of the extensive experimental data presented in Fig. 7 yields values for

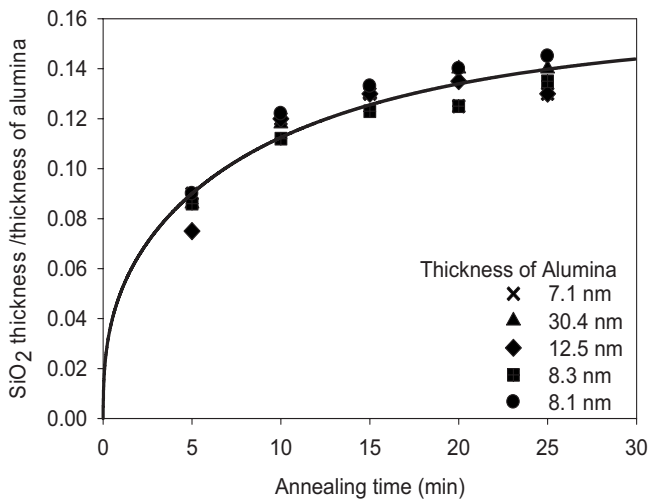


FIG. 7. Thickness of the SiO₂ film formed when Al₂O₃ is used as the high-*k* material. The oxide thickness is depicted as a function of annealing time in inert ambient at 1 bar and annealing temperature of 500 °C. The experimental data from Chowdury (Ref. 43) are fitted to determine the diffusivity of the oxygen species. The parameters used are $D_{(O_2, SiO_2)}=25.0 \text{ nm}^2/\text{s}$ (Ref. 36), $k_{(SiO_2)}=0.035 \text{ nm/s}$ (Ref. 36), $h=2.8 \times 10^7 \text{ nm/s}$ (Ref. 28), and $C_0=11.7 \text{ molecules/nm}^3$.

$D_{O, Al_2O_3}=0.075 \text{ nm}^2/\text{s}$ and $\alpha=0.82$. This value of diffusivity is within the range of oxygen diffusivities in alumina calculated and reported by Nabatame *et al.*³⁹ by using ¹⁸O tracer and secondary ion mass spectroscopy. Such calculations show that a relatively simple macroscopic model can indeed be used to predict the annealing-induced growth of interfacial oxide and can provide important guidelines for a controlled interfacial SiO₂ formation.

C. Alumina film as diffusion barrier for hafnia on silicon substrates

HfO₂ has generated considerable attention as a promising alternative to SiO₂ for future CMOS devices. However, annealing of these films in oxygen atmospheres may lead to the formation of uncontrolled SiO₂ interface layers. Since the formation of such an interface layer imposes limitations on scaling the equivalent oxide thickness of HfO₂-based layers, suppression and control of this layer are important. It has been reported that amorphous alumina can be used as a diffusion barrier layer between a HfO₂ thin film and the Si substrate.⁴⁰ Figure 8 shows predicted silicon oxide interlayer thickness as a function of the annealing time of HfO₂(4 nm)Al₂O₃ (variable nm as shown)/Si structures in 1 bar of pure oxygen at 900 °C. For comparison purposes, the silicon oxide interlayer thicknesses for 4 nm thick HfO₂/Si and 4 nm thick Al₂O₃/Si structures annealed in 1 bar oxygen at 900 °C are also included. The Al₂O₃ film has a very low oxygen diffusivity. Moreover, the Al₂O₃/Si interface remains abrupt even after 60 min of postdeposition annealing in oxygen ambient.⁴⁰ Figure 8 shows that the interfacial SiO₂ growth decreases with increasing Al₂O₃ diffusion barrier thickness. For example, we predict a SiO₂ thickness of 0.2

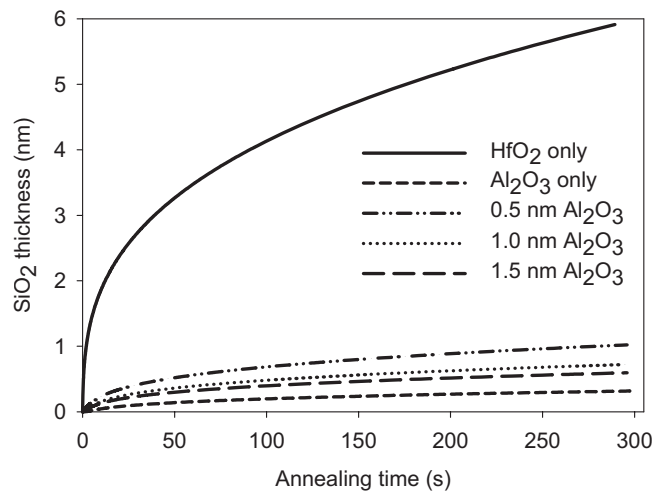


FIG. 8. Predicted thickness of the interfacial SiO₂ film as a function of annealing time at 1 bar O₂ and 900 °C for the different Al₂O₃ barrier layer thicknesses shown. Thickness of HfO₂=4.0 nm. The parameters used are $D_{(O_2, HfO_2)}=201.6 \text{ nm}^2/\text{s}$ (Refs. 30 and 35), $D_{(O_2, Al_2O_3)}=0.45 \text{ nm}^2/\text{s}$ (Refs. 38), $D_{(O_2, SiO_2)}=2.5 \times 10^4 \text{ nm}^2/\text{s}$ (Ref. 36), $k_{(SiO_2)}=641.8 \text{ nm/s}$ (Ref. 36), $h=2.8 \times 10^7 \text{ nm/s}$ (Ref. 28), $C_0=0$, and $C_{\text{bulk}}=0.0062 \text{ molecules/nm}^3$ (calculated by using ideal gas equation).

nm after 100 s annealing of Al₂O₃/Si at 900 °C, and this is substantially lower than the interlayer SiO₂ thickness of 4 nm predicted for the same annealing process of HfO₂/Si structures with no Al₂O₃ barrier interlayer. Since the HfO₂ layer may be relatively transparent to oxygen, oxygen diffusion through the Al₂O₃ layer significantly affects the interfacial SiO₂ thickness. Kundu *et al.*⁴⁰ speculated that the diffusing oxygen species are molecular in nature. When the Al₂O₃ interlayer is used, we predict an initial fast interfacial layer growth stage followed by a slow one, which is similar to that observed when only HfO₂ is considered as the high-*k* layer. However, the SiO₂ interfacial growth is significantly suppressed when an Al₂O₃ interlayer was present. These results show that although Si oxidation at the Si interface takes place by the same apparent mechanism as that when no interlayer is present, the reaction process of oxygen with silicon is constrained by the limited availability of oxygen at the Al₂O₃/SiO₂ interface. This decelerates the growth rate. However, to apply Al₂O₃ as the oxygen barrier for the high-*k* gate fabrication process, the EOT of the dielectric stack (HfO₂/Al₂O₃/SiO₂) should be approximately equal to 1 nm.³⁸ From Fig. 8 for 4.0 nm thick HfO₂ dielectric layer, if we use a 0.5 nm thick Al₂O₃ barrier layer to suppress the interfacial SiO₂ formation in order to maintain interface thickness EOT less than 1.0 nm, the thickness of interfacial oxide should be <0.15 nm. This implies that the annealing time at 900 °C should be less than 5 s. Based on such findings, the presence of Al₂O₃ on Si is indeed predicted to be an effective diffusion barrier layer that limits the thickness of the SiO₂ interfacial layer, which is in good agreement with reported experimental data.^{24,41,42} Yet, there may be a limited range of thermal processing conditions for which Al₂O₃ can act as an effective barrier layer.

IV. CONCLUSION

A diffusion-reaction model has been developed and proposed to study the SiO₂ interfacial layer growth at high-*k* material structures/Si interfaces over a range of thermal annealing conditions in inert and/or oxygen ambient. The predicted thickness of the interfacial SiO₂ layer formed is shown to be a function of temperature, annealing time, and the presence of a barrier interlayer. The interfacial SiO₂ formation upon annealing in O₂ is comprised of two stages: a fast initial stage followed by a slower self-limiting one. The slow self-limiting oxidation rate is likely a consequence of reduced availability of molecular oxygen at the high-*k* structure/SiO₂ interface. A comparison between our theoretical predictions and available experimental data shows that the proposed model satisfactorily describes the process of the interfacial oxide layer growth. Alumina is predicted to be an efficient barrier to oxygen diffusion, which is in agreement with published data. This has implications on the limitation of the thickness of the intermediate layer, which in turn de-

termines the overall dielectric constant and, therefore, the overall capacitance.

Although the theoretical predictions presented and discussed above are based on values of diffusivity, rate constant, and mass transfer coefficient taken mostly from the literature, this work does demonstrate that unsteady-state diffusion-reaction phenomena in high-*k* nanostructures can be quantitatively studied with physicochemical models like the ones proposed and solved here. Furthermore, experimental data and such models can contribute to the determination of unknown important parameters.

ACKNOWLEDGMENTS

The authors would like to thank Andreas A. Linninger from the University of Illinois at Chicago for informative and useful discussions during the development of the theoretical model. Partial financial support was provided by the Motorola Foundation.

*takoudis@uic.edu

- ¹A. I. Kingon, J. P. Maria, and S. K. Streiffer, *Nature (London)* **406**, 1032 (2000).
- ²S. H. Lo, D. A. Buchanan, Y. Taur, and W. Wang, *IEEE Electron Device Lett.* **18**, 209 (1997).
- ³E. Y. Wu, J. H. Stathis, and L.-K. Han, *Semicond. Sci. Technol.* **15**, 425 (2000).
- ⁴D. A. Muller, T. Sorsch, S. Moccio, F. H. Baumann, K. Evans-Lutterodt, and G. Timp, *Nature (London)* **399**, 758 (1999).
- ⁵H. F. Luan, S. J. Lee, C. H. Lee, S. C. Song, Y. L. Mao, Y. Senzaki, D. Robert, and D. L. Kwong, *Tech. Dig. - Int. Electron Devices Meet.* 1999, 141.
- ⁶G. B. Alers, D. J. Werder, Y. Chabal, H. C. Lu, E. P. Gusev, E. Garfunkel, T. Gustafsson, and R. S. Urdahl, *Appl. Phys. Lett.* **73**, 1517 (1998).
- ⁷S. A. Campbell, D. C. Gilmer, W. Xiao-Chuan, M.-T. Hsieh, H.-S. Kim, W. L. Gladfelter, and J. Yan, *IEEE Electron Device Lett.* **44**, 104 (1997).
- ⁸M. Copel, M. Gribelyuk, and E. Gusev, *Appl. Phys. Lett.* **76**, 436 (2000).
- ⁹W.-J. Qi, R. Nieh, B. H. Lee, L. Kang, Y. Jeon, K. Onishi, T. Ngai, S. Banerjee, and J. C. Lee, *Tech. Dig. - Int. Electron Devices Meet.* 1999, 145.
- ¹⁰G. D. Wilk, R. M. Wallace, and J. M. Anthony, *J. Appl. Phys.* **87**, 484 (2000).
- ¹¹G. D. Wilk, R. M. Wallace, and J. M. Anthony, *J. Appl. Phys.* **89**, 5243 (2001).
- ¹²R. M. C. de Almeida and I. J. R. Baumvol, *Surf. Sci. Rep.* **49**, 1 (2003).
- ¹³Y. S. Lin, R. Puthenkovilakam, and J. P. Chang, *Appl. Phys. Lett.* **81**, 2041 (2002).
- ¹⁴E. P. Gusev, M. Copel, E. Cartier, I. J. R. Baumvol, C. Krug, and M. A. Gribelyuk, *Appl. Phys. Lett.* **76**, 176 (2000).
- ¹⁵D. A. Buchanan, E. Gusev, E. Cartier, H. Okorn-Schmidt, K. Rim, M. Gribelyuk, A. Mocuta, A. Ajmera, M. Copel, S. Guha, N. Bojarczuk, A. Callegari, C. D'Emic, P. Kozlowski, K. Chan, R. J. Fleming, P. Jamison, J. Brown, and R. Arndt, *Tech. Dig. - Int. Electron Devices Meet.* 2000, 223.
- ¹⁶A. Roy Chowdhuri and C. G. Takoudis, *Thin Solid Films* **446**, 155 (2004).
- ¹⁷B. G. Segda, M. Jacquet, and J. P. Besse, *Vacuum* **62**, 27 (2001).
- ¹⁸T. M. Klein, D. Niu, W. S. Epling, W. Li, D. M. Maher, C. C. Hobbs, R. I. Hegde, I. J. R. Baumvol, and G. N. Parsons, *Appl. Phys. Lett.* **75**, 4001 (1999).
- ¹⁹Y.-C. Kim, H.-H. Park, J. S. Chun, and W.-J. Lee, *Thin Solid Films* **237**, 57 (1994).
- ²⁰B. W. Busch, W. H. Schulte, E. Garfunkel, T. Gustafsson, W. Qi, R. Nieh, and J. Lee, *Phys. Rev. B* **62**, R13290 (2000).
- ²¹B. H. Lee, L. Kang, R. Nieh, W.-J. Qi, and J. C. Lee, *Appl. Phys. Lett.* **76**, 1926 (2000).
- ²²D. Landheer, J. A. Gupta, G. I. Sproule, J. P. McCaffrey, M. J. Graham, K. C. Yang, Z. H. Lu, and W. N. Lennard, *J. Electrochem. Soc.* **148**, G29 (2001).
- ²³A. Kumar, D. Rajdev, and D. L. Douglass, *J. Am. Ceram. Soc.* **55**, 439 (1972).
- ²⁴H. Y. Yu, N. Wu, M. F. Li, C. Zhu, B. J. Cho, D. L. Kwong, C. H. Tung, J. S. Pan, J. W. Chai, W. D. Wang, D. Z. Chi, C. H. Ang, J. Z. Zheng, and S. Ramanathan, *Appl. Phys. Lett.* **81**, 3618 (2002).
- ²⁵U. Brossmann, R. Wurschum, U. Sodervall, and H.-E. Schaefer, *J. Appl. Phys.* **85**, 7646 (1999).
- ²⁶A. S. Foster, F. Lopez Gejo, A. L. Shluger, and R. M. Nieminen, *Phys. Rev. B* **65**, 174117 (2002).
- ²⁷V. V. Kharton, A. A. Yaremchenko, E. N. Naumovich, and F. M. B. Marques, *J. Solid State Electrochem.* **4**, 243 (2000).
- ²⁸B. E. Deal and A. S. Grove, *J. Appl. Phys.* **36**, 3770 (1965).
- ²⁹H. Itoh, M. Nagamine, H. Satake, and A. Toriumi, *Microelectron. Eng.* **48**, 71 (1999).
- ³⁰S. Ferrari and G. Scarel, *J. Appl. Phys.* **96**, 144 (2004).
- ³¹H. Shimizu, K. Kita, K. Kyuno, and A. Toriumi, *Jpn. J. Appl. Phys., Part 1* **44**, 6131 (2005).
- ³²S. Ferrari and M. Fanciulli, *J. Phys. Chem. B* **110**, 14905 (2006).

- ³³I. J. R. Baumvol, C. Krug, F. C. Stedile, F. Gorris, and W. H. Schulte, *Phys. Rev. B* **60**, 1492 (1999).
- ³⁴S. V. Pantankar, *Numerical Heat Transfer and Fluid Flow* (McGraw-Hill, New York, 1980), p. 25.
- ³⁵C.-L. Liu, *Phys. Status Solidi B* **233**, 18 (2002).
- ³⁶R. M. C. de Almeida, S. Gonçalves, I. J. R. Baumvol, and F. C. Stedile, *Phys. Rev. B* **61**, 12992 (2000).
- ³⁷R. R. Razouk, L. N. Lie, and B. E. Deal, *J. Electrochem. Soc.* **128**, 2214 (1981).
- ³⁸L. Date, Z. M. Rittersma, D. Massoubre, Y. Ponomarev, F. Roozeboom, D. Pique, L. van-Autryve, S. Van Elshocht, and M. Caymax, *IEEE/SEMI Advanced Semiconductor Manufacturing Conference*, 133 (2003).
- ³⁹T. Nabatame, T. Yasuda, M. Nishizawa, M. Ikeda, T. Horikawa, and A. Toriumi, *Jpn. J. Appl. Phys., Part 1* **42**, 7205 (2003).
- ⁴⁰M. Kundu, N. Miyata, T. Nabatame, T. Horikawa, M. Ichikawa, and A. Toriumi, *Appl. Phys. Lett.* **82**, 3442 (2003).
- ⁴¹M. Park, J. Koo, J. Kim, H. Jeon, C. Bae, and C. Krug, *Appl. Phys. Lett.* **86**, 252110 (2005).
- ⁴²R. Katamreddy, R. Inman, G. Jursich, A. Soulet, and C. Takoudis, *Appl. Phys. Lett.* **89**, 262906 (2006).
- ⁴³A. Roy Chowdhuri, Ph.D. thesis, University of Illinois, 2003.